Light-Harvesting Properties of a Subphthalocyanine Solar Absorber Coupled to an Optical Cavity

Victoria Esteso, Laura Caliò, Hilario Espinós, Giulia Lavarda, Tomás Torres, Johannes Feist, Francisco J. García-Vidal, Giovanni Bottari,* and Hernán Míguez*

Herein, both from the experimental and theoretical point of view, the optical absorption properties of a subphthalocyanine (SubPc), an organic macrocycle commonly used as a sunlight harvester, coupled to metallic optical cavities are analyzed. How different electronic transitions characteristic of this compound and specifically those that give rise to excitonic (Q band) and charge transfer (CT band) transitions couple to optical cavity modes is investigated. It is observed that whereas the CT band couples weakly to the cavity, the Q band transitions show evidence of hybridization with the photon eigenstates of the resonator, a distinctive trait of the strong coupling regime. As a result of the different coupling regimes of the two electronic transitions, very different spectral and directional light-harvesting features are observed, which for the weakly coupled CT transitions are mainly determined by the highly dispersive cavity modes and for the strongly coupled Q band by the less angle-dependent exciton-polariton bands. Modeling also allows discriminating parasitic from productive absorption in each case, enabling the estimation of the expected losses in a solar cell acting as an optical resonator.

V. Esteso, L. Caliò, H. Espinós, H. Míguez
Instituto de Ciencia de Materiales de Sevilla (CSIC-US)
41092 Sevilla, Spain
E-mail: h.miguez@csic.es

G. Lavarda
Departamento de Química Orgánica
Universidad Autónoma de Madrid
28049 Madrid, Spain

T. Torres, G. Bottari
Departamento de Química Orgánica and Institute for Advanced Research in Chemical Sciences (IAdChem) Universidad Autónoma de Madrid, Spain and IMDEA-Nanociencia, Campus de Cantoblanco
28049 Madrid, Spain
E-mail: giovanni.bottari@uam.es

J. Feist, F. J. García-Vidal
Departamento de Física Teórica de la Materia Condensada and Condensed Matter Physics Center (IFIMAC)
Universidad Autónoma de Madrid
28049 Madrid, Spain

The ORCID identification number(s) for the author(s) of this article can be found under https://doi.org/10.1002/solr.202100308.

1. Introduction

Within the context of organic materials for optoelectronics, subphthalocyanines (SubPcs), aromatic macrocycles with a cone-shaped structure, constitute a particularly interesting family of compounds.[1] These derivatives present an intense optical absorption in the UV-vis region of the solar spectrum and high fluorescence quantum yields, a rich redox chemistry, and excellent charge transport capabilities, physicochemical properties that can be finely tuned through structural modifications.[2] It is precisely their potential in fields such as molecular photovoltaics,[3,4] light-emitting diodes (LEDs),[5,6] nonlinear optics (NLO),[7,8] and electronics[9,10] that has triggered a large amount of research in the controlled modification of the electronic structure of SubPcs, usually achieved by functionalization with ligands and/or atoms at their peripheral positions.[11] In the case of SubPcs used as sunlight absorbers, their light-harvesting spectrum is usually tailored to present a rich structure of absorption bands.[12] Recently, spectral control over the absorption of SubPcs has been achieved by means of their integration in a solar cell that also behaves as an optical resonator, in which the metallic contacts play the role of highly reflecting mirrors.[13] The performance of this novel photovoltaic device depends on the specific coupling of the SubPc intrinsic electronic transitions to the photon eigenmodes of the optical cavity. In fact, this reconfiguration of the electronic and optical states of the cell led to a reduction of the photon energy losses by effectively decreasing the bandgap of the light harvesting material while, simultaneously, lowering the electron driving force and hence the charge transfer losses. In this context, understanding how the different electronic transitions in a SubPc couple to the photon eigenmodes of a solar cell that also behaves as an optical resonator is an important issue that deserves to be addressed.

Herein, we investigate how two electronically different transitions, namely, a charge transfer (CT) band and an excitonic Q band, of a SubPc embedded within an optical cavity respond to variations in the resonant modes of such a cavity. In good agreement with our modeling, we observe that excitonic Q bands display strong coupling effects, which imply a significant hybridization of the photon cavity modes with the SubPc electronic transitions to form polaritonic states.[14–16] In contrast, the

usually less intense CT bands undergo weak coupling, which results in a very different spectral and directional light-harvesting response. Also, by modeling the system under analysis, we can discriminate the productive absorption occurring in the SubPc layer from the parasitic one due to the presence of metallic films in the structure, which allows us to estimate the potential optical losses that may occur in a light-harvesting device devised as an optical resonator.

2. Results and Discussion

The configuration of the SubPc-containing optical cavities herein studied is shown in **Figure 1**a. In brief, a 20 nm thick film of poly(vinyl alcohol) (PVA) was spin cast onto a 35 nm thick layer of silver (Ag) sputtered on a glass substrate (see Supporting Information for details). On top of this layer, dispersions of SubPc **1** (structure in the inset of Figure 1a) in polystyrene (PS) (35 wt% concentration) were spin cast, obtaining layers of different thicknesses, followed by the deposition of a 20 nm thick PVA layer. While PS is required to ensure the film flatness, the PVA coating contributes to improve the thin film uniformity. Finally, the ensemble was covered by a thermally evaporated layer of silver (35 nm thick) to obtain a Fabry–Pérot optical resonator. While silver, PVA, and PS were chosen to assure the optical quality of the resulting layered structure (i.e., absence of diffuse scattering due to irregularities), SubPc **1** was selected due to its peculiar optical features. **1** is a perfluorinated SubPc, previously

Figure 1. Fabry–Pérot resonator structure and optical constants. a) Schematic representation of the structure of the Fabry–Pérot resonators built for this work. The inset shows the chemical structure of SubPc-TCBD-aniline **1**. b) Absorptance (red line) of a film containing a 35 wt% SubPc-TCBD-aniline **1** dispersed in PS. Dashed lines show the simulated reflectance spectra of the cavities designed to couple their respective first order mode to the Q band (black dashed line, with cavity thickness L_C^1 of 140 nm) and to the CT band (gray dashed line, with cavity thickness L_C^2 of 94 nm). c) Experimentally determined refractive index (n) and absorption coefficient (κ) (i.e., real and imaginary part of the complex refractive index) of the SubPc-TCBD-aniline **1**/PS film as a function of photon wavelength (bottom) and energy (top).

studied by some of us,[17,18] substituted at its axial position by a tetracyanobuta-1,3-diene (TCBD)-aniline group. Figure 1b displays the absorptance spectrum of a thin film of **1** in which the characteristic visible excitonic band at around 600 nm resulting from the singlet-singlet S0 → S1 transition (Q band), described by Gouterman's four-orbital model,[19,20] coexists with a CT band at around 480 nm resulting from the electron donor–acceptor coupling between the TCBD (the acceptor) and the aniline (the donor) moieties.[17]
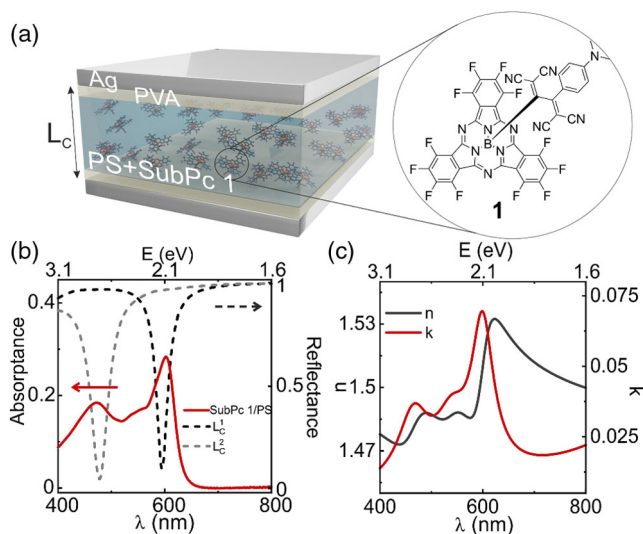
To study the coupling of optical cavity modes to the different intrinsic absorption bands of SubPc-TCBD-aniline **1**, cavities with different thicknesses (L_C) were fabricated to ensure that the frequency of the first order optical resonance ($\omega_C = c\pi/L_C n$, with c and n being the speed of light in vacuum and the cavity refractive index, respectively) matches either the excitonic or the CT absorption band of the SubPc-TCBD-aniline 1 containing film. The spectral position of these modes can be readily identified as minima in the reflectance spectrum of the cavities (dashed lines in Figure 1b, corresponding to $L_C^1 = 140$ nm and $L_C^2 = 94$ nm).

These spectra are calculated considering the effective refractive index n of the **1**/PS composite at $\lambda = 700$ nm (in the transparency region of the film), which is extracted from the experimental determination of the optical constants, plotted in Figure 1c (a complete description of the method used to determine these constants is provided as Supporting Information as well as the $n(\lambda)$ and $\kappa(\lambda)$ curves for the Ag and PVA layers in the ensemble; see Figure S1 and S2, Supporting Information, respectively). It is worth noting that, among the excitonic bands present in the spectrum of **1**, we focus exclusively on the effect of the optical resonator on the SubPc Q band as the SubPc Soret absorption occurs at too high energies to be relevant for sunlight-harvesting applications.
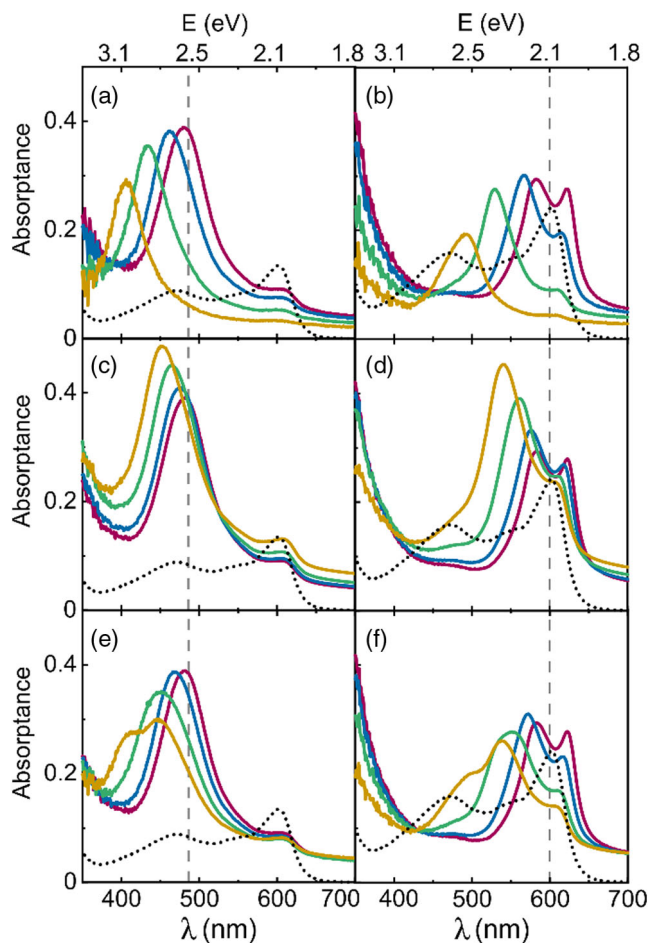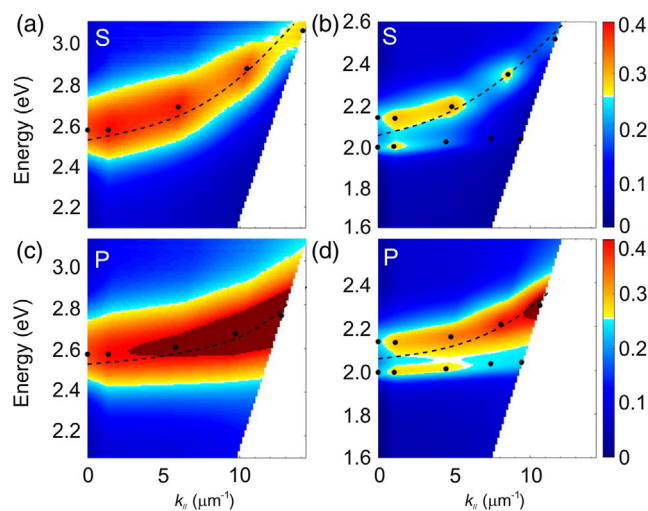
First, we analyzed the absorptance (A) of SubPc-TCBD-aniline **1**/PS films coupled to optical resonators. In this context, absolute reflectance (R) and transmittance (T) measurements at variable direction of incidence θ (from 0° to 66° with respect to the surface normal) and polarization (S or TE, and P or TM) were conducted. We used a double goniometer configuration (Universal Measurement Accessory attached to a Cary 5000 spectrophotometer), which allowed us to rotate independently the sample and detector and hence select arbitrary incidence and collection angles.

Absorptance for each angle of incidence was estimated using the expression $A = 1 - T - R$. In **Figure 2**, we display the resulting absorptance spectra for the two different SubPc-TCBD-aniline-containing resonators at different angles and polarizations of incident light.

For one resonator (i.e., $L_C^2 = 94$ nm), the first order optical cavity mode coincides spectrally with the CT band (Figure 2a,c,e), whereas for the other (i.e., $L_C^1 = 140$ nm) it matches the excitonic Q band (Figure 2b,d,f). In each case, the spectrum of a bare SubPc-TCBD-aniline/PS film of similar thickness (i.e., 94 or 140 nm) is plotted for the sake of comparison (black dotted line). Absorptance of unpolarized light is estimated by averaging the experimental results attained for the S and P polarizations at each θ. Also, by plotting the absorptance intensity maps versus photon energy and the parallel component of the wavevector $\mathbf{k}_\parallel$, $\mathbf{k} = \mathbf{k}_\parallel + \mathbf{k}_\perp$, we obtain the dispersion relations for each resonator and for both polarizations (**Figure 3**).[21]

Figure 2. Polarization (a,b) S-polarized, c,d) P-polarized, and e,f) unpolarized light) and angle-dependent (violet line = 6°, blue line = 26°, green line = 46°, yellow line = 66°) absorptance spectra of optical resonators coupled to the CT (left) and the Q (right) absorption bands of SubPc-TCBD-aniline **1** dispersed in PS. Dotted lines indicate the absorptance spectrum of a SubPc-TCBD-aniline **1**/PS film. Vertical dashed lines indicate the reflectance minimum for cavities with L_C of 94 (left) and 140 nm (right).

These measurements reveal some interesting features. On one hand, the coupling between **1** and the two optical cavity modes gives rise to significant modifications of the light absorption properties of the sandwiched SubPc-TCBD-aniline/PS film. On the other hand, the interaction between the electronic transitions involved in either the CT or Q bands with the photon cavity modes presents substantial qualitative differences, which are discussed in what follows. Coupling between optical cavity modes and CT bands yields a single, well-defined, enhanced absorption peak (Figure 2a,c,e) that closely follows the dispersion of the cavity modes (dashed lines in Figure 3a,c). This is characteristic of *weak coupling*, a regime in which electrons, holes, or excitons interact weakly with the resonant photon states of the cavity; i.e., the energy exchange between them takes longer than the excited state dephasing and decay or recombination lifetime (for charges) and the characteristic lifetime (for photons). In practical terms, weak coupling gives rise to light absorption enhancement at those photon frequencies matching the optical cavity resonances.[22] On the other hand, the interplay between

Figure 3. Energy dispersion bands resulting for the coupling with the CT (left) and the Q (right) absorption bands of SubPc-TCBD-aniline **1**. Absorptance intensity maps versus photon energy (y-axis) and $\mathbf{k}_\parallel$ (x-axis) for a,b) S- and c,d) P-polarized light. In both cases, the dashed line corresponds to the cavity mode, and black dots represent calculated absorptance maxima at different angles (i.e., 0°, 6°, 26°, 46° and 66°).

photon states and the excitonic transitions associated with the Q band gives rise to a splitting of that band (Figure 2b,d,f). Each of these two new absorption maxima shows up at frequencies that do not correspond either to the optical resonances of the cavity or to the intrinsic absorption maxima of the embedded SubPc-TCBD-aniline **1**. Furthermore, the energy dispersion relation shows an absorption splitting of ≈150 meV (Figure 3b,d). This particular feature is distinctive of a system undergoing *strong coupling*, a regime in which the energy exchange rate between charges and photons is faster than their respective relaxation times.[23] On these premises, the system can no longer be described by the eigenstates of its individual components. Instead, hybrid light-matter states, also known as polaritons, are the quasiparticles that now provide an adequate picture of the properties of the ensemble.[14–16]

The absorption splitting arising from the anticrossing of the upper and lower polaritonic energy bands displayed in Figure 3b, d is commonly referred to as Rabi splitting and its width, ΔE, is given by[24]

$$\Delta E = \hbar\Omega_R = 2\hbar g = \mathbf{E} \times \mathbf{\mu}^{g\to e} \tag{1}$$

where $\hbar$ is the reduced Planck constant, Ω_R is the Rabi frequency (i.e., the rate at which energy is exchanged between the photonic mode and the electronic transition), $\hbar g$ is the coupling strength, $\mathbf{E}$ is the cavity mode electric field, and $\mathbf{\mu}^{g\to e}$ is the dipole moment of the transition between the molecule ground and excited state occurring at a frequency ω_0. From the magnitude of the cavity field of frequency ω_C

$$|\mathbf{E}| = \sqrt{\frac{\hbar\omega_c}{\varepsilon_0 V_c}} \tag{2}$$

The relation between the magnitude of $\mathbf{\mu}^{g\to e}$, μ, and the oscillator strength of such a transition, f[25]

$$\mu^2 = \frac{3\hbar e^2}{2m\omega_0}f \tag{3}$$

and assuming that $\omega_C = \omega_0$ and that N molecules effectively contribute to the coupling, the coupling strength can then be expressed as

$$\hbar g = \sqrt{\frac{3\hbar^2 e^2}{2m\varepsilon_0}\frac{N}{V_C}f} \tag{4}$$

where e and m are the electron charge and mass, respectively, ε_0 is the vacuum dielectric permittivity, and V_C is the effective cavity mode volume. Please note that, among all randomly oriented SubPc-TCBD-aniline molecules in the film, only those for which $\boldsymbol{\mu}^{g\rightarrow e}$ is not perpendicular to $\mathbf{E}$ will be involved in the coupling. Also, for the case of a broad absorption band, like the Q band herein studied, f, which is a dimensionless number directly proportional to the absorption intensity, is not univocally defined. The effects of structural disorder and spectral inhomogeneous broadening of the electronic transition have been discussed in the literature.[26,27] It has been concluded that the absorption peak splitting, and hence the coupling strength estimated from it, is independent of the homogeneous or inhomogeneous character of the oscillator strength and is still proportional to $\sqrt{N/V_C}f$ as stated in Equation (4).

Based on this description, the coupling behavior observed for the CT and Q bands of **1** may be attributed to the different contributions of their respective oscillator strengths because in the two cases both the intensity and mode volume of the photon resonances involved are very similar, as it will be explicitly shown later, and also the concentration of molecules potentially involved in the coupling. Whereas the Q band in **1** is the result of highly localized excitations with large f, CT bands are typically broader and less intense, hence presenting smaller f, as it can be seen in both the absorptance spectrum of the SubPc-TCBD-aniline/PS film (Figure 1b) and the spectral dependence of the extinction coefficient κ (Figure 1c). This implies that CT bands will be more likely to undergo weak rather than strong coupling even in the presence of intense optical resonances, as observed. This is not a fundamental limitation as if by any means (i.e., by modifying the nature of the ligand) the oscillator strength of the transitions responsible for the appearance of CT bands is enlarged, strong coupling effects could be observed. For that to occur, the Rabi energy splitting should be larger than the average of the full widths at half maximum of the bare molecule electronic transition, $\Delta\omega_{CT}$, and the cavity resonance, $\Delta\omega_C$:[28]

$$\Delta E = \hbar\Omega_R = \frac{\Delta\hbar\omega_{CT} + \Delta\hbar\omega_c}{2} \tag{5}$$

which, in our case, sets a threshold of $\Delta E_{CT} > 490$ meV. A similar calculation for the Q band ($\Delta\hbar\omega_Q$) yields a threshold of $\Delta E_Q > 100$ meV, lower than the splitting we actually observe. It is worth noting that although we are dealing here with an intramolecular CT band, some predictions can be made on the potential observation of strong coupling to intermolecular CT states, characteristic of heterojunction organic photovoltaic devices. As intermolecular absorption bands are typically less intense than intramolecular ones, strong coupling to those electronic
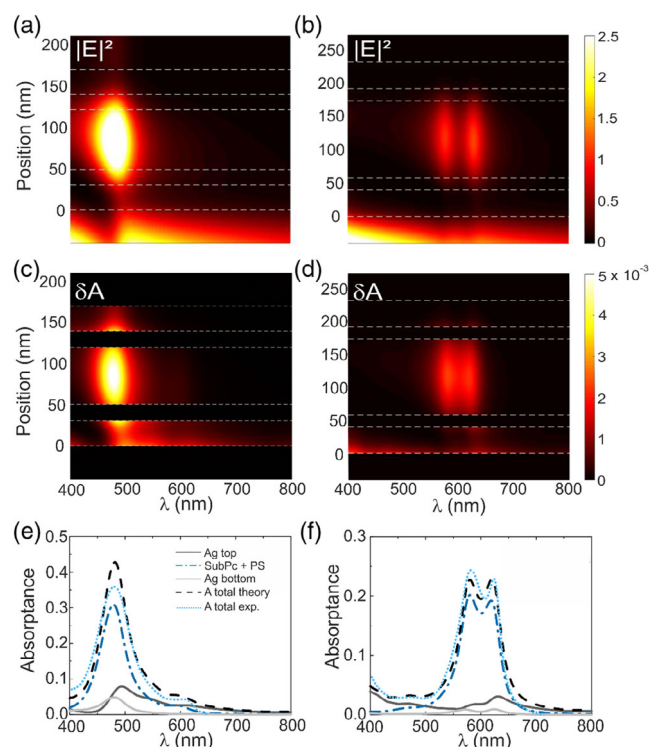
transitions should be even less likely. It should also be taken into account that the magnitude of the coupling can be tuned by controlling, if possible, the orientation of the molecules. Therefore, it has been shown that the coupling of the excitonic transitions of an organic tetracene crystal with cavity modes switches between weak and strong coupling as the relative orientation of the corresponding transition dipole moment with respect to the direction of the light electric field in the cavity is varied.[29]

Further insight into the mechanism by which absorption is enhanced or suppressed at selected spectral and spatial regions for the two coupling regimes is gained by simulating the optical response of **1**. To do so, we use a classical electrodynamics approximation based on the transfer matrix method (TMM),[30] which takes as input the experimentally determined thickness and optical constants of each layer present in the resonator (see Figure S1 and S2, Supporting Information). This approach has been successfully applied to simulate collective strong coupling effects,[31] such as the ones herein described, in which quantum features may be disregarded. Apart from reproducing the angular and polarization-dependent reflectance, transmittance and absorption intensity maps (simulated spectra are available in the Supporting Information; see Figure S4 and S5, Supporting Information), whose dispersion fully agrees with the experimentally attained, our model allows visualizing the spatial and spectral profiles of the electric field intensity, $|\mathbf{E}(\mathbf{r})|^2$, for each kind of coupling, as shown in the maps plotted in **Figure 4**a, b, which have been calculated assuming a plane wave impinging normally on the resonators ($\mathbf{k}_\parallel = 0$).

In both cases, the single-node spatial distribution of $|\mathbf{E}(\mathbf{r})|^2$ is characteristic of the coupling with a first order cavity mode. For the case of the strongly coupled Q band (Figure 4b), the mode splitting, responsible for the opening of the absorption energy gap, may be clearly seen. Moreover, our model allows calculating the luminous power absorbed in regions of volume V presenting a nonzero imaginary part of the dielectric constant ($\varepsilon_i = 2n\kappa$), P_A, as derived from Maxwell equations

$$P_A = \frac{1}{2}\omega\varepsilon_0(2n\kappa)\int_V |\mathbf{E}(\mathbf{r})|^2 d\mathbf{r} \tag{6}$$

Normalizing P_A with respect to the incident power $P_I = \frac{1}{2}c\varepsilon_0\int_V |\mathbf{E}_0(\mathbf{r})|^2 d\mathbf{r}$, with $\mathbf{E}_0$ the incident electric field, we obtain the absorptance per unit length/volume δA. Results are plotted in Figure 4c,d. The possibility to increase optical absorption by locally enhancing $|\mathbf{E}(\mathbf{r})|^2$ in a specific region by optical design has been put into practice many times to improve the light-harvesting efficiency of solar cells or photodetectors at wavelength ranges for which absorption is low.[32,33] In fact, we observe a significant absorptance enhancement at those wavelengths and in those regions in which $|\mathbf{E}(\mathbf{r})|^2$ is maximum. Also, this approach allows discriminating the optical losses occurring at each layer in the ensemble, hence providing an estimation of parasitic (unproductive) absorption as a result of the presence of mirrors (analogous to reflecting metal contacts in a solar cell shaped as an optical resonator). Figure 4e,f displays the discriminated absorptance ($A = \int\delta A\,dz$, z being the position inside the cavity) for each of the absorbing layers in the ensemble, i.e., SubPc-TCBD-aniline film and top and bottom silver mirrors. Losses mainly occur in the top mirror, whose size is similar

Figure 4. a,b) Calculated spatial and spectral profiles of the electric field intensity $|\mathbf{E(r)}|^2$, and c,d) the absorbed luminous power P_A for the resonators under study. Left and right columns show results for the coupling with the CT and the Q bands of SubPc-TCBD-aniline **1**, respectively. Curves in (e) and (f) are the corresponding discriminated absorptance in each absorbing layer in each resonator.

to those previously used in polaritonic light-harvesting devices.[13,34] Also, please note that the spectral distribution of losses differs in both Ag mirrors, being blueshifted in the bottom one. A theoretical analysis of the dependence of parasitic and productive losses under sunlight irradiation was conducted for the cavity that is strongly coupled to the Q band for different top and bottom silver mirror thickness combinations (see Figure S7 and S8, Supporting Information). In brief, we observe that the absorptance of the SubPc-TCBD-aniline/PS layer is maximized for a combination of a thick bottom Ag layer (i.e., 40 nm) and a thin top Ag layer (i.e., 20 nm), for which strong coupling is still observed. Overall, the discriminated solar spectrum weighted absorptance (SSWA) analysis reveals that the total parasitic losses comprise between 2% and 5% for the range of representative parameters considered.

3. Conclusion

In conclusion, our results clearly show that light-matter coupling is a very powerful tool to tailor the photophysical properties of molecular solar absorbers, potentially leading to a finer control over their response in photovoltaic or photodetection devices. We have experimentally and theoretically analyzed the light-harvesting properties of a SubPc (**1**) embedded in Fabry–Pérot resonators. The results obtained show that the characteristic

electronic transitions of this compound that are responsible for their visible light absorption, namely, the excitonic (Q) and charge-transfer (CT) bands, couple in a different way to the optical cavity modes, which is a direct consequence of their different oscillator strengths. Whereas CT bands couple weakly to the cavity, and hence their absorption angular dispersion closely follows that of the cavity modes, Q band transitions show clear evidence of exciton–photon hybridization and their light-harvesting properties are determined by the dispersion of the newly formed polaritonic bands. From the point of view of the photonic design of a photovoltaic device, a cell that presents less dependence, or none, on the light incidence direction is wanted. Therefore, a strongly or, even better, an ultrastrongly coupled cell, in which light harvesting shows a low angular dispersion, would be preferable versus a weakly coupled one. This is also of relevance if a system such as the one herein studied is used as a photodetector, for which a flat angular response is also preferred. Modeling also allows us to discriminate parasitic from potentially productive absorptions in each case, enabling us to estimate the expected losses in a solar cell acting as an optical resonator. We reckon that these results add an important contribution to unravel how different electronic transitions of a chromophore embedded in a polaritonic solar cell, or, more generally, in a solar cell shaped as an optical resonator, differently contribute to sunlight harvesting and determine the angular response of the device.

Supporting Information

Supporting Information is available from the Wiley Online Library or from the author.

Conflict of Interest

The authors declare no conflict of interest.

Data Availability Statement

Research data are not shared.

Keywords

excitonic and charge transfer bands, light harvesting, optical cavity, strong coupling, subphthalocyanine

[1] C. G. Claessens, D. González-Rodríguez, M. S. Rodríguez-Morgade, A. Medina, T. Torres, *Chem. Rev.* **2014**, *114*, 2192.

[2] P. Heremans, D. Cheyns, B. P. Rand, *Acc. Chem. Res.* **2009**, *42*, 1740.

[3] B. Verreet, B. P. Rand, D. Cheyns, A. Hadipour, T. Aernouts, P. Heremans, A. Medina, C. G. Claessens, T. Torres, *Adv. Energy Mater.* **2011**, *1*, 565.

[4] K. Cnops, B. P. Rand, D. Cheyns, B. Verreet, M. A. Empl, P. Heremans, *Nat. Commun.* **2014**, *5*, 3406.

[5] D. D. Díaz, H. J. Bolink, L. Cappelli, C. G. Claessens, E. Coronado, T. Torres, *Tetrahedron Lett.* **2007**, *48*, 4657.

[6] G. E. Morse, M. G. Helander, J. F. Maka, Z. H. Lu, T. P. Bender, *ACS Appl. Mater. Interfaces* **2010**, *2*, 1934.

[7] C. G. Claessens, D. González-Rodríguez, T. Torres, G. Martín, F. Agulló-López, I. Ledoux, J. Zyss, V. R. Ferro, J. M. De La García Vega, *J. Phys. Chem. B* **2005**, *109*, 3800.

[8] H. M. Kim, B. R. Cho, *J. Mater. Chem.* **2009**, *19*, 7402.

[9] G. E. Morse, T. P. Bender, *ACS Appl. Mater. Interfaces* **2012**, *4*, 5055.

[10] G. De La Torre, G. Bottari, U. Hahn, T. Torres, *Struct. Bond.* **2010**, *135*, 1.

[11] H. Gommons, T. Aernouts, B. Verreet, P. Heremans, A. Medina, C. C. Claessens, T. Torres, *Adv. Funct. Mater.* **2009**, *19*, 3435.

[12] B. B. Berna, B. Platzer, M. Wolf, G. Lavarda, S. Nardis, P. Galloni, T. Torres, D. M. Guldi, R. Paolesse, *Chem. Eur. J.* **2020**, *26*, 13451.

[13] V. C. Nikolis, A. Mischok, B. Siegmund, J. Kublitski, X. Jia, J. Benduhn, U. Hörmann, D. Neher, M. C. Gather, D. Spoltore, K. Vandewal, *Nat. Commun.* **2019**, *10*, 3706.

[14] P. Törmä, W. L. Barnes, *Reports Prog. Phys.* **2015**, *78*, 013901.

[15] T. W. Ebbesen, *Acc. Chem. Res.* **2016**, *49*, 2403.

[16] J. Galego, F. J. Garcia-Vidal, J. Feist, *Phys. Rev. X* **2015**, *5*, 041022.

[17] K. A. Winterfeld, G. Lavarda, J. Guilleme, M. Sekita, D. M. Guldi, T. Torres, G. Bottari, *J. Am. Chem. Soc.* **2017**, *139*, 5520.

[18] G. Lavarda, N. Bhattacharjee, G. Brancato, T. Torres, G. Bottari, *Angew. Chem. Int. Ed.* **2020**, *59*, 21224.

[19] M. Gouterman, *J. Mol. Spectrosc.* **1961**, *6*, 138.

[20] M. Gouterman, G. H. Wagnière, L. Snyder, *J. Mol. Spectrosc.* **1963**, *11*, 108.

[21] All reflectance, transmittance and absorptance spectra versus angle of incidence and polarization, as well as the corresponding energy versus $k_\parallel$ dispersion relations extracted from them, are provided as Supporting Information (see Figure S4–S6, Supporting Information).

[22] N. P. Sergeant, A. Hadipour, B. Niesen, D. Cheyns, P. Heremans, P. Peumans, B. P. Rand, *Adv. Mater.* **2012**, *24*, 728.

[23] D. G. Lidzey, D. D. C. Bradley, M. S. Skolnick, T. Virgili, S. Walker, D. M. Whittaker, *Nature* **1998**, *395*, 53.

[24] H. L. Luk, J. Feist, J. J. Toppari, G. Groenhof, *J. Chem. Theory Comput.* **2017**, *13*, 4324.

[25] I. Pelant, J. Valenta, *Oxford Univ. Press* **2012**, ISBN 978-0-19-958833-6.

[26] R. Houdré, R. P. Stanley, M. Ilegems, *Phys. Rev. A* **1996**, *53*, 2711.

[27] S. Gambino, M. Mazzeo, A. Genco, O. Di Stefano, S. Savasta, S. Patanè, D. Ballarini, F. Mangione, G. Lerario, D. Sanvitto, G. Gigli, *ACS Photonics* **2014**, *1*, 1042.

[28] M. Hertzog, M. Wang, J. Mony, K. Börjesson, *Chem. Soc. Rev.* **2019**, *48*, 937.

[29] A. M. Berghuis, V. Serpenti, M. Ramezani, S. Wang, J. Gómez Rivas, J. Gómez Rivas, *J. Phys. Chem. C* **2020**, *124*, 12030.

[30] Y. Zhu, D. J. Gauthier, S. E. Morin, Q. Wu, H. J. Carmichael, T. W. Mossberg, *Phys. Rev. Lett.* **1990**, *64*, 2499.

[31] F. Herrera, J. Owrutsky, *J. Chem. Phys.* **2020**, *152*, 100902.

[32] A. Jiménez-Solano, J. F. Galisteo-López, H. Míguez, *J. Phys. Chem. Lett.* **2018**, *9*, 2077.

[33] H. A. Atwater, A. Polman, *Nat. Mater.* **2010**, *9*, 205.

[34] E. Eizner, J. Brodeur, F. Barachati, A. Sridharan, S. Kéna-Cohen, *ACS Photonics* **2018**, *5*, 2921.